



Facial distortion due to chronic inflammation of unknown cause in a cat

Lynelle R Johnson¹ , Sarah A Vidal², Kelsey D Brust², M Kevin Keel³ and Michele A Steffey⁴

Journal of Feline Medicine and Surgery Open Reports
1–6

© The Author(s) 2020

Article reuse guidelines:

sagepub.com/journals-permissions

DOI: 10.1177/2055116920957200

journals.sagepub.com/home/jfmsopenreports

This paper was handled and processed by the American Editorial Office (AAFP) for publication in *JFMS*



Abstract

Case summary An 8-year-old neutered male indoor cat was presented for evaluation of a year-long history of swelling over the bridge of the nose that extended from the subcutaneous tissue of the right upper eyelid to the dorsum of the skull. Intermittent regression of the mass lesion was reported with antibiotic or corticosteroid therapy; however, progressive swelling, malaise and hiding behavior persisted. CT revealed an aggressive osteolytic mass lesion in the right and left nasal cavities and extending into the frontal sinuses. Rhinoscopy using a 2.8 mm rigid telescope revealed somewhat normal-appearing turbinates rostrally and ventrally on the left side, with turbinate destruction on the right. After obtaining a biopsy from the right side of the nasal cavity, thick material filling the entire nasal cavity was visible caudally and was extracted endoscopically from a rostral approach. Surgical biopsy of the dorsal nasal bridge resulted in protrusion of inspissated material from the incision site. Rhinoscopic exploration revealed that the material extended into both frontal sinuses. Following extensive debridement and medical therapy, marked resolution of facial asymmetry was achieved.

Relevance and novel information Facial distortion is often considered suggestive of a neoplastic process; however, it can also be seen with fungal and mycobacterial infections, and, in this case, an inflammatory condition of unknown etiology. In this cat, aggressive intervention and debridement of necrotic debris resulted in substantial bony remodeling of the skull and return to normal activity levels.

Keywords: Chronic rhinosinusitis; facial asymmetry; rhinoscopy; rhinotomy

Accepted: 31 July 2020

Introduction

Facial distortion and bony asymmetry in the cat are often related to a neoplastic process, with carcinoma, lymphoma and sarcoma reported most commonly.¹ Fungal infections are also known to result in bony remodeling centered around the nasal cavity (cryptococcosis) or the oral cavity (aspergillosis), and other fungi such as *Sporothrix* species and systemic mycoses can result in facial deformity.^{2–4} Finally, atypical bacteria and mycobacterium can be involved in proliferative soft tissue and bony lesions in the cat.^{5,6}

In most cases, identification of the underlying etiology of facial deformity can be achieved with blood tests, advanced imaging, aspiration cytology and microbiology, or wedge biopsy; however, some cases elude ready identification of the cause. Inflammation in the nasal cavity and frontal sinuses is sometimes related to an

identifiable cause such as a foreign body or tooth root disease; however, chronic rhinosinusitis, the most common disorder affecting the upper respiratory tract of

¹Department of Medicine and Epidemiology, School of Veterinary Medicine, University of California-Davis, Davis, CA, USA

²William R Pritchard Veterinary Medical Teaching Hospital, Davis, CA, USA

³Department of Pathology, Microbiology and Immunology, School of Veterinary Medicine, University of California-Davis, Davis, CA, USA

⁴Department of Surgical and Radiological Sciences, School of Veterinary Medicine, University of California-Davis, Davis, CA, USA

Corresponding author:

Lynelle R Johnson DVM, PhD, DACVIM (Small Animal Internal Medicine), Department of Medicine and Epidemiology, School of Veterinary Medicine, University of California-Davis, Davis, CA 95616, USA

Email: lrjohnson@ucdavis.edu



Creative Commons Non Commercial CC BY-NC: This article is distributed under the terms of the Creative Commons

Attribution-NonCommercial 4.0 License (<https://creativecommons.org/licenses/by-nc/4.0/>) which permits non-commercial use, reproduction and distribution of the work without further permission provided the original work is attributed as specified on the SAGE and Open Access pages (<https://us.sagepub.com/en-us/nam/open-access-at-sage>).

cats,⁷ is a particularly challenging disease process that has evaded adequate description of the etiopathogenesis of disease. Multiple studies using invasive and molecular diagnostic testing have failed to identify a treatable condition, which interferes with effective therapeutic intervention. This case illustrates the utility of repeat diagnostic imaging and intervention to investigate and resolve facial deformity associated with an inflammatory condition of unknown etiology.

Case description

An 8-year-old indoor, neutered male domestic shorthair cat was presented to the William R Pritchard Veterinary Medical Teaching Hospital at the University of California, Davis, for evaluation of a non-painful, generalized expansion of the nasal bridge that was first noted 1 year previously. Initially, the owners observed subcutaneous tissue swelling of the right eyelid resulting in epiphora, and this swelling gradually expanded across the nasal bridge. They reported good appetite but general malaise and increased hiding behavior over the course of the year. Past history was unremarkable except for chronic sneezing that was managed with 1 mg chlorpheniramine each evening.

During the year prior to presentation, the cat had seen multiple veterinarians, including board-certified internists, ophthalmologists and oncologists. A complete blood count (CBC), chemistry panel and urinalysis were normal, cryptococcal antigen titer was negative and thoracic radiographs demonstrated a moderate bronchial pattern with focal alveolar infiltrates consistent with mucus plugging. Fine-needle aspiration cytology of the eyelid mass and several biopsy samples of the region across the nasal bridge 9–10 months prior to referral revealed marked histiocytic and mild neutrophilic and lymphocytic inflammation suggestive of an inflammatory nodule. The swelling partially regressed intermittently with combinations of oral antibiotics (marbofloxacin, doxycycline, azithromycin), intralesional steroid injections, and oral or ophthalmic corticosteroids.

Two months prior to referral, nasal CT revealed a centrally hypodense, peripherally contrast-enhancing soft tissue mass dorsal to the bridge of nose, with a defect in the dorsal aspect of the maxilla and nasal bones. A biopsy was obtained externally from between the eyes and revealed severe necrotizing and suppurative inflammation. Bacterial and fungal cultures of the biopsy sample were negative. Fluconazole was initiated, but swelling of the nasal bridge progressed, the suture site began to ooze bloody fluid and a smaller lump developed on the right upper eyelid, prompting referral to the Oncology Service at UC Davis. Physical examination revealed marked widening of the nasal bridge with an oozing biopsy site centrally, facial distortion and an eyelid mass on the right upper lid (Figure 1). The remainder of the physical examination was within normal limits. Feline leukemia virus/feline immunodeficiency virus and repeat cryptococcal



Figure 1 An 8-year-old neutered male domestic shorthair cat had marked widening of the nasal bridge with an oozing biopsy site centrally, facial distortion and an eyelid mass on the right upper lid on presentation to the Oncology Service

antigen tests were negative. Abdominal ultrasound revealed splenomegaly and aspirates suggested possible emerging hepatosplenic lymphoma or splenic reactivity. DNA was extracted from coverslip slides from the splenic aspirate and T-cell molecular clonality PCR resulted in reproducible broad polyclonal humps, indicative of a reactive or hyperplastic process. Fluconazole (50 mg), marbofloxacin (18.75 mg) and doxycycline (50 mg) were discontinued.

Ten days later, the cat was referred to the Internal Medicine Service. No weight loss or inappetence were reported, and the history was negative for coughing, diarrhea, vomiting, nasal discharge and polyuria/polydipsia. Travel history revealed that the cat had moved from New Jersey to Virginia to Tennessee and then California 2.5 years ago. On physical examination, the cat was normothermic and eupneic. Non-painful swelling of the nasal bridge began 5 mm caudal to the nostrils and extended to the top of the head, as seen previously. It was ~2 cm in width and coalesced with an area of swelling near the medial canthus of the right eye. There was a circumferential area of alopecia (1 cm in diameter) above the swelling from a previous biopsy. Bilateral nasal airflow was present, oral examination was unremarkable, and local lymph nodes were normal in size and consistency. A grade III/VI left parasternal heart murmur was auscultated with normal rhythm and femoral pulses.

Differential diagnoses for facial asymmetry and swelling included fungal infection (*Aspergillus* species, a non-encapsulated *Cryptococcus* species, *Sporothrix* species,

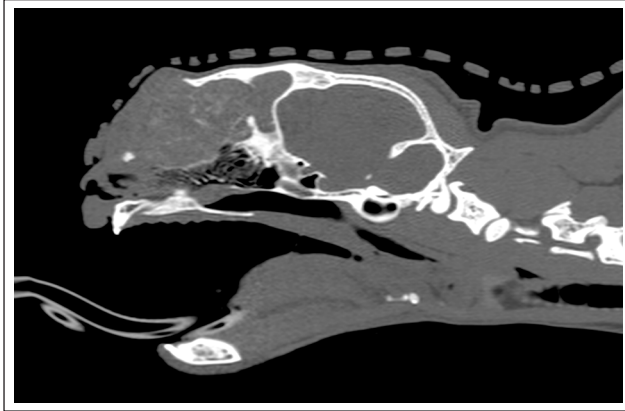


Figure 2 Parasagittal pre-contrast CT reconstruction of the skull reveals a dorsally expansile and lytic mass lesion

other fungal species), atypical mycobacterial infection and a poorly exfoliating, slow-growing neoplastic process. The owner agreed to repeat diagnostic testing.

A pre-anesthetic echocardiogram showed no evidence of organic heart disease, and the murmur was ascribed to dynamic right ventricular outflow tract obstruction. A CBC revealed a normocytic, normochromic, non-regenerative anemia (hematocrit [Hct] 18.8%, reticulocytes 52,300/ μ l) consistent with anemia of chronic disease and normal white blood count (13,700/ μ l; reference interval [RI] 4500–14,000/ μ l) characterized by normal neutrophil numbers (3209/ μ l; RI 2000–9000/l) and mild lymphocytosis (9854/ μ l; RI 1000–7000/ μ l) with normal cytologic morphology. Whole blood was submitted for *Mycoplasma haemofelis/haemocanis* quantitative PCR and was negative. A chemistry panel revealed hyperbilirubinemia (0.4 mg/dl; RI 0–0.2 mg/dl) with normal liver enzymes, and urinalysis showed a urine specific gravity of 1.050 with bilirubinuria (3 mg/dl).

A cross-match and blood typing was performed prior to anesthesia for CT and endoscopy. A packed cell volume of 12% was detected after induction, which necessitated a transfusion with 1 unit of packed red blood cells. A second unit was administered approximately 3 h into the procedure to provide continued cardiovascular support. A 0.6 mm axial CT of the skull pre- and post-contrast revealed a large, soft tissue-attenuating, heterogeneously contrast-enhancing mass predominately within the right nasal cavity and extending into the left nasal cavity and frontal sinuses (Figure 2; see also Video 1 in the supplementary material). Thin mineral striations were present throughout the mass. There was severe patchy osteolysis of the left and right nasal bones and the nasal portion of the frontal bones, as well as partial osteolysis of the right orbital plate, frontal processes of the left and right maxillary bones, and frontal sinus septum, resulting in severe expansile dorsal and right-sided

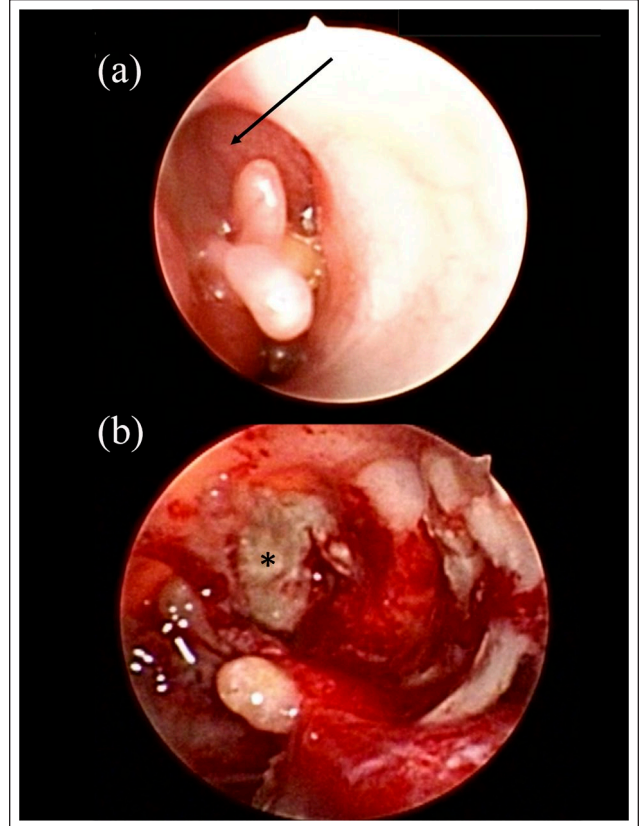


Figure 3 Rhinoscopy of the right nasal cavity revealed moderate turbinate destruction (arrow, a). (b) Post-biopsy: thick mucoid material (*) was visible caudally

facial distortion. There was a focal region of lysis of the nasal portion of the left frontal bone with dorsal soft tissue swelling.

Rhinoscopy demonstrated a normal appearance to the ventral turbinates on the left side and mild turbinate swelling dorsally. On the right side, mucus and turbinate destruction was noted dorsally, as well as a yellow polypoid mass lesion (Figure 3). Biopsy of the lesion revealed mats of caseous material caudally that were debrided with 2 mm cup biopsy forceps. A 2 cm skin incision was made over the rostral aspect of the dorsal nasal swelling and resulted in exudation of a similar thick, yellow, caseous substance from the site (Figure 4). This material filled the dorsal expansile compartment of the nasal cavity and both frontal sinuses, and was removed by rhinoscopically assisted debridement using a 3 mm curette and flushing (see Video 2 in the supplementary material). Intranasal and sinus material was submitted for histopathology, bacterial, fungal and mycoplasmal culture, and mycobacterial culture and PCR. The resulting cavity was copiously lavaged and visually inspected with the rigid telescope to ensure removal of all gross disease, and the skin incision was closed with a buried interrupted subcuticular pattern with 4-0 monocryl and two external cruciate skin sutures



Figure 4 Incision into the mass effect on the dorsal nasal bridge resulted in exudation of thick mucoid material



Figure 5 A 6 cm segment of a 5Fr red rubber tube was sutured into the cavity that resulted from debridement of inspissated material from the frontal sinuses

of 4-0 nylon. A 6 cm section of a 5Fr red rubber tube was placed transdermally into the cavity to allow venting of air and was affixed to the skin with a finger trap pattern using 3-0 nylon (Figure 5). Buprenorphine (0.02 mg/kg) was administered intramuscularly twice post-procedure for pain control.

The cat was discharged on amoxicillin–clavulanic acid (13 mg/kg) q12h pending culture results and piroxicam (0.21 mg/kg) q24h for 1 week then q48h for 1 month. Piroxicam was chosen for its anti-inflammatory and pain relief properties based on clinical experience with long-term use in cats diagnosed with nasal inflammation post-biopsy. Histopathology of samples from both nasal cavities and from the dorsal nasal bridge was reported as necrotic debris characterized by pale eosinophilic to basophilic, amorphous material with scattered karyorrhectic nuclear and cellular debris, and abundant degenerate neutrophils. Sunburst-like foci composed of radiating, clear clefts (cholesterol) and small, polygonal, polarizing structures were distributed multifocally within the necrotic material. Spicules of shattered turbinate structures were scattered among the tissue fragments. The respiratory mucosa was variably hyperplastic and the submucosa expanded by edema and infiltrated by multifocal to regionally extensive aggregates of lymphocytes, plasma cells and neutrophils. All sections were similarly affected by a marked, multifocal to regionally extensive inflammatory process characterized by

lymphocytes, plasma cells and fewer neutrophils. Special stains (periodic acid–Schiff and Grocott methenamine silver) were negative for organisms, while Giemsa and Gram staining revealed rare extracellular rods and cocci, and bacterial cultures (aerobic, anaerobic and mycoplasma) were negative. Mycobacterium quantitative PCR and culture from nasal tissue/debris were negative, and fungal culture was negative.

Four days after discharge, the red rubber stent was removed by the referring veterinarian when the eye was noted to be swollen, and sutures were removed at 14 days. Repeat CBC revealed mild anemia (Hct 28%; RI 29–48%) and persistent lymphocytosis (9840/ μ l; RI 1200–8000/ μ l). Renal parameters remained within the RI (blood urea nitrogen 19 mg/dl [range 14–36 mg/dl]; creatinine 1.0 mg/dl [range 0.6–2.4 mg/dl]), and both bilirubinemia and bilirubinuria had resolved. Medications were discontinued after 1 month. One year after intervention, marked improvement in remodeling of the skull had occurred (Figure 6), although no additional imaging was performed, and the cat was reported to be more interactive and energetic than in the previous 2 years.

Discussion

Facial deformity in the cat is most commonly associated with nasal neoplasia or fungal infection.^{1,4,8,9} The most common infectious disease process resulting in facial



Figure 6 One year follow-up image of the 9-year-old neutered male domestic shorthair reveals marked resolution of facial swelling

deformity is cryptococcosis, although *Sporothrix* species and phaeohyphomycoses should also be considered as causes for a mass lesion, along with systemic mycotic agents such as *Histoplasma capsulatum* and *Blastomyces dermatitidis*. Most of these fungi are readily apparent on cytologic preparations, although non-encapsulated species of *Cryptococcus* can be more challenging to identify and can result in a false-negative antigen titer.¹⁰ The newly recognized *Aspergillus felis* is commonly associated with orbital and paranasal soft tissue involvement with mass lesions in the nasal cavity, nasopharynx and oral cavity, as well as orbital lysis, but the *Aspergillus* species can usually be visualized histologically.^{2,11} Atypical bacterial, including mycobacterium and *Neisseria*-like organisms, can also lead to a similar presentation; however, organisms are more typically identified in aspirates or biopsy samples and can be grown in culture, albeit using a specialized medium.^{5,6,12} While chronic rhinosinusitis is one of the most common nasal conditions of cats,⁷ and is often associated with internal destruction of turbinates, bony proliferation and external remodeling of the skull are not typical.

In this case, multiple cultures were negative for both typical and atypical organisms, and histopathology of the

tissue revealed primarily necrosis and chronic inflammation. It is possible that chronic antibiotic therapy suppressed growth of potential pathogens; however, the etiology of this cat's destructive and proliferative facial lesion remains unclear. It is possible that an unrecognized pathogen gained access to the frontal sinuses via the nasal route with local extension, as has been proposed for *A felis*, as well as other fungal organisms.² Given that the swelling originated near the medial canthus of the right eye, a penetrating foreign body might have entered via that approach and traveled toward the frontal sinuses; however, no such substance was identified with imaging or histopathology. Nevertheless, this remains a potential etiology as it is not uncommon for foreign material to migrate through a site and exit the body, leaving a trail of inflammation in its path. We did not have access to previous biopsy slides to compare the type of cellular infiltrate present in order to elucidate the progression of the inflammatory process.

While the material removed from the nasal cavity and the dorsal nasal bridge was similar to that found in chronic rhinosinusitis, it is unusual that the cat did not display nasal discharge, which is one of the top historical findings in this syndrome. Antihistamines are sometimes recommended for cats with sneezing and nasal discharge based on their use in humans with rhinitis, and long-term use was employed in the cat of this report. It is possible that use of antihistamines might have masked the typical signs of rhinitis by drying of secretions and lessening nasal discharge. This might also have contributed to inspissation of mucus and impaction of this material in the nasal cavity and frontal sinus, resulting in overwhelming inflammation and the expansile mass effect. The etiology of the inflammation remains unclear.

CT suggested a mass effect on the dorsum of the nose and the release of necrotic, inspissated material during surgical biopsy was unexpected. The exposure provided through the surgical site allowed effective debridement of necrotic and inflamed material as far back as the frontal sinuses and was likely instrumental in providing relief in this cat. Combining a more traditional external surgical approach with concurrent internal endoscopic visualization of the nasal cavity during debridement was useful in this case. Rhinoscopic visual inspection of the nasal and sinus cavities provided magnification and access into crevices that allowed clinicians to identify and surgically target focal areas of residual disease that could not be seen from the surgical approach, ultimately providing a more complete debridement. Despite the lack of detected pathogens, antibiotic therapy was used in the management of this cat given the surgical exploration and extensive cavity that resulted following debridement, which could be susceptible to harboring infection. After 1 month of

amoxicillin–clavulanic acid, no further antibiotic treatment has been required in the year since debridement. We consider it highly unlikely that an undetected fungal or atypical bacteria would have responded so well to therapy. Non-steroidal anti-inflammatory treatment was provided for pain relief, as well as control of inflammation, and likely contributed to the improvements in facial remodeling noted over time. This agent was used cautiously (daily then every other day) to avoid gastrointestinal or renal side effects and was well tolerated over the month of therapy.

Conclusions

In this case, a multimodal approach to therapy incorporating advanced imaging, pathology, and endoscopic, surgical and medical treatment resulted in a successful outcome. Cooperation and collaboration among multiple services provided a complete evaluation of the underlying condition and ultimately led to resolution of clinical disease in this unusual case with chronic inflammation of indeterminant cause.

Acknowledgements We would like to thank the hospital staff for their contributions to diagnostic testing in this case.

Conflict of interest The authors declared no potential conflicts of interest with respect to the research, authorship, and/or publication of this article.

Funding The authors received no financial support for the research, authorship, and/or publication of this article.

Ethical approval This work involved the use of non-experimental animals only (including owned or unowned animals and data from prospective or retrospective studies). Established internationally recognized high standards ('best practice') of individual veterinary clinical patient care were followed. Ethical approval from a committee was therefore not necessarily required.

Informed consent Informed consent (either verbal or written) was obtained from the owner or legal custodian of all animal(s) described in this work (either experimental or non-experimental animals) for the procedure(s) undertaken (either prospective or retrospective studies). For any animals or humans individually identifiable within this publication, informed consent (either verbal or written) for their use in the publication was obtained from the people involved.

ORCID ID Lynelle R Johnson  <https://orcid.org/0000-0002-5331-5626>

Supplementary material Supplementary material for this article is available online.

References

- Mukaratirwa S, van der Linde-Sipman JS and Gruys E. **Feline nasal and paranasal sinus tumours: clinicopathological study, histomorphological description and diagnostic immunohistochemistry of 123 cases.** *J Feline Med Surg* 2001; 3: 235–245.
- Barrs VR, Halliday C, Martin P, et al. **Sinonasal and sino-orbital aspergillosis in 23 cats: aetiology, clinicopathological features and treatment outcomes.** *Vet J* 2012; 191: 58–64.
- Lloret A, Hartmann K, Pennisi MG, et al. **Rare opportunistic mycoses in cats: phaeohyphomycosis and hyalohyphomycosis: ABCD guidelines on prevention and management.** *J Feline Med Surg* 2013; 15: 628–630.
- Pennisi MG, Hartmann K, Lloret A, et al. **Cryptococcosis in cats: ABCD guidelines on prevention and management.** *J Feline Med Surg* 2013; 15: 611–618.
- Carr SV, Martin PA, Keyes SL, et al. **Nasofacial infection in a cat due to a novel bacterium in Neisseriaceae.** *JFMS Open Rep* 2015; 1. DOI: 10.1177/2055116915597240.
- O'Brien CR, Malik R, Globan M, et al. **Feline leprosy due to *Mycobacterium lepraemurium*.** *J Feline Med Surg* 2017; 19: 737–746.
- Ferguson S, Smith KC, Welsh CE, et al. **A retrospective study of more than 400 feline nasal biopsy samples in the UK (2006–2013).** *J Feline Med Surg* 2020; 22: 736–743.
- Schoenborn WC, Wisner ER, Kass PP, et al. **Retrospective assessment of computed tomographic imaging of feline sinonasal disease in 62 cats.** *Vet Radiol Ultrasound* 2003; 44: 185–195.
- Sfiligoi G, Théon AP and Kent MS. **Response of nineteen cats with nasal lymphoma to radiation therapy and chemotherapy.** *Vet Radiol Ultrasound* 2007; 48: 388–393.
- Tintelnot K, Adler S, Bergmann F, et al. **Disseminated cryptococcoses without cryptococcal antigen detection.** *Mycoses* 2000; 43: 203–207.
- Barrs VR, Beatty JA, Dhand NK, et al. **Computed tomographic features of feline sino-nasal and sino-orbital aspergillosis.** *Vet J* 2014; 201: 215–222.
- Gunn-Moore DA, McFarland SE, Brewer JI, et al. **Mycobacterial disease in cats in Great Britain: I. Culture results, geographical distribution and clinical presentation of 339 cases.** *J Feline Med Surg* 2011; 13: 934–944.